Journal of Physics: Conference Series

PAPER • **OPEN ACCESS**

On the carbuncle instability of the HLLE-type solvers

To cite this article: Zhijun Shen *et al* 2019 *J. Phys.: Conf. Ser.* **1290** 012026

IOP Conf. Series: Journal of Physics: Conf. Series **1290** (2019) 012026 doi:10.1088/1742-6596/1290/1/012026

On the carbuncle instability of the HLLE-type solvers

Zhijun Shen, Jian Ren, Xia Cui

Laboratory of Computational Physics, Institute of Applied Physics and Computational Mathematics, P. O. Box 8009-26, Beijing 100088, China

E-mail: shen_zhijun@iapcm.ac.cn, ren_jian@iapcm.ac.cn, cui_xia@iapcm.ac.cn

Abstract. The carbuncle phenomenon is a numerical instability that affects the numerical capturing of shock waves when low-dissipative upwind scheme is used. This paper investigates shock instabilities of the HLLE-type methods for the Euler equations under the strong shock interaction, where the HLLE-type methods include the HLLE, HLLC, HLLEM, HLLCM and HLLEC Riemann solvers with specific wavespeed estimates. Based on a matrix stability analysis for two dimensional steady shocks, a new factor to influence carbuncle phenomenon is pointed out and the choice of the signal velocity plays an important role. A numerical flux function with wave velocity estimates which can crisply resolve shocks seems to be vulnerable to the shock anomalies even if the numerical fluxes to be regarded to be free from the carbuncle phenomenon. A suggestion to the choice of the wave speed is proposed when calculating strong shock wave problems.

1. Introduction

Shock-capturing Godunov schemes have become a mainstay in aerospace calculations and also in a range of other fields such as astrophysics, space physics, fusion and several others. This is due to their low numerical dissipation, their high level of robustness, and their ability to exactly capture discontinuities. However, such upwind Riemann solvers have their own peculiar flaws. One of the well-known flaws is the carbuncle phenomenon.

The carbuncle phenomenon is a numerical instability that affects the numerical capturing of shock waves. It was first reported by Peery and Imlay [11] when they calculated a high speed flow interacting with a blunt body. Quirk [12] found that the carbuncle instability was also related to the even-odd decoupling problem when he simulated planar moving shocks. Since the discovery of this pathology, one may associate the carbuncle instability with several other instabilities involving the propagation of shocks on a multidimensional computational mesh. For example, a shock moving on a multidimensional mesh with skewed mesh lines [3] or uneven mesh spacing [13] [20] will also show deficiencies. In all such circumstances, overcoming the carbuncle instability also contributes to overcome all these other deficiencies associated with strong shocks moving on multi-dimensional meshes.

In the procedure of seeking the cause of shock instability, the first stability analysis was offered by Quirk [12] who realized that the instability was triggered by an exact representation of the linearly degenerate intermediate waves. Riemann solvers like the HLLE solver, which does not resolve intermediate waves, are always stable, while low dissipative Riemann solvers like the Roe-type solver were unstable unless a large dose of dissipation was introduced by using Harten's fix [7]. Quirk constructed a hybrid method to cure shock instability. It switches to a more dissipative Riemann solver in the vicinity of shock wave to efficiently dissipate intermediate waves, and restores low dissipative scheme, like Roe Riemann solver, on other domains. Such healing has a hypotheses that the high dissipative scheme is always stable in calculations.

Sanders et al.[14] noticed that the dimension by dimension extension of one-dimensional upwind schemes to the multidimensional equations of gas dynamics often leads to poor results when computing strong shocks. They showed that this failure is an instability which is the result of inadequate crossflow dissipation implied by strictly upwind schemes. Further studies show that the carbuncle phenomenon mainly arises from the perpendicular cell face of shock wave [9],[15] [19]. Adding appropriate amount of dissipation on these faces is conductive to damp out the carbuncle phenomenon. Related numerical algorithms involve the modification of linear shear wave. Two concrete Riemann solvers are the HLLCM scheme [16] and HLLEC scheme [19]. They originate from the unstable HLLC [18] and the HLLEM flux functions [5], but illustrate very good stability since shear waves in original schemes are smeared or deleted.

Only a few works realized that the normal dissipation is also source of instability. Kitamura et al. [8] made some comparisons to a slew of Riemann solvers and found that "there are at least two kinds of shock instabilities at work: one is one-dimensional (1-D) mode and the other is multidimensional mode". If a scheme is unstable in 1-D, then it remains unstable in two dimensional calculation. However, there are also some puzzling behaviors for the above conclusion. Actually, some schemes in [8] (EC-Roe(α = 0.2),AUSMPW+, RoeM2) are 1D unstable but 2D stable (see Table 2 in [8]). In [19], the HLLEC flux has similar performance, see Table 3 in [19]. Therefore corresponding connection between 1D and 2D instability is not clear.

In this paper, we discuss the stability of HLLE-type numerical fluxes, including HLLC, HLLCM, HLLEM and HLLEC. One of the common characters of these numerical fluxes is that the right-going and left-going wave velocities need to be given artificially. There are many methods to estimate the speeds. The most popular approach is to estimate them directly. Davis [2] proposed an exceedingly simple algorithm by comparing the maximum and minimum characteristic velocities of both states. He further suggested that one could estimate the shock velocities from an intermediate state based on the Roe average. This was implemented as a wavespeed algorithm due to Einfeldt et al.'s work[5]. For the HLLC flux, Batten et al. [1] showed that Einfeldt et al.'s estimates can resolve contact waves exactly and guarantee the method is positively conservative. Especially, the algorithm "has proved extremely robust and can yields the exact velocity for isolated shocks", and thus is recommended for practical computations [1]. The classical HLLEM adopts Einfeldt et al.'s wave algorithm naturally, and it also possesses above discontinuity resolving properties after selecting the appropriate contact velocity, see [10].

However, the HLLC and HLLEM Riemann solvers were found to be unstable to the carbuncle instability due to their full family of waves construction. While the HLLCM flux [16] is a modification of the HLLC flux and the HLLEC [19] is one of the HLLEM flux. The main modification focus on smearing or deleting the linear shear wave. According to the analysis in [16] and [19], the HLLCM method and HLLEC method do not suffer from carbuncle instability. In particular, in almost all literatures, the HLLE scheme is believed to be carbuncle free.

In this paper, we will report some numerical experiments with strong steady shock waves, in which instability phenomena occur for the three so-called 'stable' numerical fluxes: the HLLE, HLLCM and HLLEC schemes equipped with Einfeldt et al.'s wavespeed algorithm. As a simple cure, Davis's wavespeed algorithm is adopted and greatly improves the stability of numerical calculations. A matrix stability analysis is put forward to validate the finding.

The outline of the paper is as follows. In Section 2, the governing equations and some Riemann solvers are introduced. An unstable phenomenon is described in Section 3, the computing effects using two different wavespeed estimates are illustrated in the section. In Section 4, a linear matrix stability analysis is proposed, and the stability of two choices is described. In particular, an extreme counterexample is given to illustrate the limitation of the two classical wavespeed

IOP Conf. Series: Journal of Physics: Conf. Series **1290** (2019) 012026 doi:10.1088/1742-6596/1290/1/012026

algorithms. Finally, the conclusions are summarized in Section 5.

2. Governing equations and numerical methods

The governing equations for inviscid flow in two dimensions are as follows:

$$\frac{\partial \mathbf{U}}{\partial t} + \frac{\partial \mathbf{F}(\mathbf{U})}{\partial x} + \frac{\partial \mathbf{G}(\mathbf{U})}{\partial y} = 0, \tag{1}$$

where the state vector and flux vectors are

$$\mathbf{U} = \begin{bmatrix} \rho \\ \rho u \\ \rho v \\ \rho E \end{bmatrix}, \qquad \mathbf{F}(\mathbf{U}) = \begin{bmatrix} \rho u \\ \rho u^2 + p \\ \rho uv \\ \rho Eu + pu \end{bmatrix}, \qquad \mathbf{G}(\mathbf{U}) = \begin{bmatrix} \rho v \\ \rho uv \\ \rho v^2 + p \\ \rho Ev + pv \end{bmatrix},$$

where ρ, p, E are the fluid density, pressure and total energy respectively, and $\mathbf{u} = (u, v)$ is the fluid velocity. The equation of state is in the form

$$p = (\gamma - 1)\rho e = (\gamma - 1)\rho \left[E - \frac{1}{2}(u^2 + v^2) \right],$$

where γ is the specific heat ratio and e is the specific internal energy.

For simplicity assume that the boundaries of the computational domain are aligned with the coordinate directions x and y. Consider a typical finite volume or computational cell $\Omega_{i,j}$ of dimensions $\Delta x \times \Delta y$. To each intercell boundary there corresponds a numerical flux.

A semi-discrete finite volume method to solve (1) reads

$$\frac{d\mathbf{U}_{i,j}}{dt} = -\frac{\mathbf{H}_{i+1/2,j} - \mathbf{H}_{i-1/2,j}}{\Delta x} - \frac{\mathbf{H}_{i,j+1/2} - \mathbf{H}_{i,j-1/2}}{\Delta y}, \tag{2}$$

where the numerical fluxes $\mathbf{H}_{i+1/2,j}$ and $\mathbf{H}_{i,j+1/2}$ are approximate intercell ones of $\mathbf{F}(x_{i+1/2}, y_j)$ and $\mathbf{G}(x_i, y_{j+1/2})$ respectively. They can be obtained by many methods. In this paper, we concentrate on the HLLE-type Riemann solvers.

2.1. Some approximate Riemann solvers

When discretizing the equations (1), Riemann solver is an important ingredient in numerical methods. The HLL Riemann solver [6] is one of lots of Riemann solvers [17]. It approximates the solution of Riemann problem with two waves propagating at speeds of S_L and S_R. They are the lower and upper bounds for the physical signal speeds with which the information of the initial discontinuity is transported. Given the initial conserved states $\mathbf{U}_L$ and $\mathbf{U}_R$ of a Riemann problem, the numerical flux of the HLL approximate Riemann solver can be expressed as

$$\mathbf{H}_{HLL} = \frac{S_R^+ \mathbf{F}_L - S_L^- \mathbf{F}_R + S_R^+ S_L^- (\mathbf{U}_R - \mathbf{U}_L)}{S_R^+ - S_L^-}, \tag{3}$$

with $S_L^- = \min(S_L, 0)$ and $S_R^+ = \max(S_R, 0)$. $\mathbf{F}_L$ and $\mathbf{F}_R$ are fluxes on the left and right sides.

To satisfy the entropy and the positivity conditions, Einfeldt et al.[5] suggested adequate bounds by making use of the Roe-averaged eigenvalues,

$$S_L = \min(u_L - a_L, \hat{u} - \hat{a}), \quad S_R = \max(u_R + a_R, \hat{u} + \hat{a}), \tag{4}$$

where a_L and a_R are the sound speeds of the left and the right states. The superscript $\hat{}$ denotes the Roe-averaged values throughout this paper. With the wavespeed estimates, the HLL flux is also called HLLE scheme. It needs to point out that the HLLE flux has too much dissipation and has difficulty to simulate practical problems. Many modifications have done to retain the shear wave and entropy wave.

2.2. HLLEM and HLLEC schemes

The HLLEM scheme [5] is an modified scheme of the HLLE flux, which improves the resolution of contact discontinuity by reusing the information of contact discontinuity in terms of modifying the intermediate state. The numerical flux function of the HLLEM scheme can be written by

$$\mathbf{H}_{HLLEM} = \mathbf{H}_{HLLE} - \frac{S_R^+ S_L^-}{S_R^+ - S_L^-}(\delta_2 \hat{\alpha}_2 \hat{\mathbf{r}}_2 + \delta_3 \hat{\alpha}_3 \hat{\mathbf{r}}_3), \tag{5}$$

where $\hat{\mathbf{r}}_k$ correspond the right eigenvectors of the flux Jacobian $\hat{\mathbf{A}}$ evaluated at the intermediate states $\hat{\mathbf{U}}$. The wave strengths $\hat{\alpha}_k$ are the approximate values of the projection from $\mathbf{U}_R - \mathbf{U}_L$ onto $\hat{\mathbf{r}}_k$, i.e.,

$$\mathbf{U}_R - \mathbf{U}_L = \sum_{k=1}^{4} \hat{\alpha}_k \hat{\mathbf{r}}_k.$$

δ_k are the anti-diffusion coefficients defined by Park et al. [10],

$$\delta_2 = \delta_3 = \frac{\hat{a}}{|\hat{u}| + \hat{a}}, \tag{6}$$

which has resolve the stationary contact discontinuity exactly.

However, two main problems have been reported for this scheme. One is multidimensional shock instability and another is nonexistence of strong receding flows. The HLLEC flux is a modification of the HLLEM one proposed by Xie et al. [19],

$$\mathbf{H}_{HLLEC} = \mathbf{H}_{HLLE} - \frac{S_R^+ S_L^-}{S_R^+ - S_L^-}\delta_2 \hat{\alpha}_2 \hat{\mathbf{r}}_2. \tag{7}$$

In this formula, the shear wave $\delta_3 = 0$ has been dropped off but the contact wave keeps unchanged. In [19], the HLLEC flux is regarded as free from shock instability.

2.3. HLLC-type schemes

The HLLC method [18] is considered to be the most preferred finite difference method because of its simplicity and ability to capture discontinuities accurately. In the Riemann solver, four constant states, which can be denoted from left to right $\mathbf{U}_L, \mathbf{U}_L^*, \mathbf{U}_R^*, \mathbf{U}_R$, are separated by signal velocities S_L and S_R and contact velocity S_*. The flux function can be expressed by

$$\mathbf{H}_{HLLC} = \begin{cases} \mathbf{F}_L, & \text{if} \quad S_L \geq 0, \\ \mathbf{F}_L + S_L(\mathbf{U}^*_{HLLC,L} - \mathbf{U}_L), & \text{if} \quad S_L < 0 \leq S_*, \\ \mathbf{F}_R + S_R(\mathbf{U}^*_{HLLC,R} - \mathbf{U}_R), & \text{if} \quad S_* < 0 < S_R, \\ \mathbf{F}_R, & \text{if} \quad S_R \leq 0, \end{cases} \tag{8}$$

where the conserved vectors in the star region are

$$\mathbf{U}^*_{HLLC,K} = \rho_K^* \begin{bmatrix} 1 \\ S_* \\ v_K \\ E_K^* \end{bmatrix} = \rho_K^* \begin{bmatrix} 1 \\ S_* \\ v_K \\ E_K^{*,1d} + \frac{1}{2}v_K^2 \end{bmatrix}, \quad \text{for} \quad K = L, R, \tag{9}$$

in which the total energy is decomposed into sums of a pure one-dimensional normal quantity $E_K^{*,1d}$ and a tangent kinetic energy $v_K^2/2$. Introduce following notations

$$\alpha_L = \rho_L(S_L - u_L), \quad \alpha_R = \rho_R(S_R - u_R),$$

then the contact velocity, density and total energy in the star region can be written as

$$S_* = \frac{\alpha_R u_R - \alpha_L u_L + p_L - p_R}{\alpha_R - \alpha_L}, \tag{10}$$

$$\rho_K^* = \frac{\alpha_K}{S_K - S_*}, \quad E_K^{*,1d} = e_K + (S_* - u_K)\left(S_* + \frac{p_K}{\alpha_K}\right), \quad K = L, R. \tag{11}$$

In order to enhance the stability, authors in [16] introduce the shear viscosity to the HLLC scheme. The modified algorithm is called the HLLCM Riemann solver and has similar flux form with (9),

$$\mathbf{H}_{HLLCM} = \begin{cases} \mathbf{F}_L, & \text{if} \quad S_L \geq 0, \\ \mathbf{F}_L + S_L(\mathbf{U}^*_{HLLCM,L} - \mathbf{U}_L), & \text{if} \quad S_L < 0 \leq S_*, \\ \mathbf{F}_R + S_R(\mathbf{U}^*_{HLLCM,R} - \mathbf{U}_R), & \text{if} \quad S_* < 0 < S_R, \\ \mathbf{F}_R, & \text{if} \quad S_R \leq 0. \end{cases} \tag{12}$$

Here, the conserved vectors in star states are

$$\mathbf{U}^*_{HLLCM,K} = \rho_K^* \begin{bmatrix} 1 \\ S_* \\ v^* \\ E^*_{HLLCM,K} \end{bmatrix} = \rho_K^* \begin{bmatrix} 1 \\ S_* \\ \frac{\alpha_R v_R - \alpha_L v_L}{\alpha_R - \alpha_L} \\ E_K^{*,1d} + \frac{1}{2}\frac{\alpha_R v_R^2 - \alpha_L v_L^2}{\alpha_R - \alpha_L} \end{bmatrix}, \quad K = L, R. \tag{13}$$

The main difference between the HLLC flux and the HLLCM flux is in the tangent velocity. The change of total energy is along with the variation of tangent velocity.

3. An instability phenomenon and cure

Shock instability of a numerical scheme means the shock front might be destroyed by a very slight perturbation. Such perturbation might come from grid, initial values, boundary conditions, even just rounding errors. In what follows, we use numerical experiments to illustrate some solution behaviors of these HLLE-type schemes.

The raw problem is a steady normal shock wave. The initial data are given by the exact Rankine-Hugoniot solution in x-direction. The upstream and downstream states are

$$\mathbf{W}_L = (\rho_L, u_L, v_L, p_L) = (1, \sqrt{\gamma}M_a, 0, 1), \quad x < 0.1, \tag{14}$$

and the downstream state is

$$\mathbf{W}_R = (\rho_R, u_R, v_R, p_R) = \left(f(M_a), \frac{\sqrt{\gamma}M_a}{f(M_a)}, 0, g(M_a)\right), x > 0.1, \tag{15}$$

where $M_a = u_L/a_L$ is the upstream Mach number of the incoming flow,

$$f(M_a) = \left(\frac{2}{\gamma+1}M_a^2 + \frac{\gamma-1}{\gamma+1}\right)^{-1}, \quad g(M_a) = \frac{2\gamma}{\gamma+1}M_a^2 - \frac{\gamma-1}{\gamma+1}.$$

The computational domain is on a rectangular one of $[0, 0.2] \times [0, 1]$ in the x-y plane, and the mesh has 20×100 uniform cells. The specific heat ratio $\gamma = 1.4$, Mach number $M_a = 20$. The signal velocity estimates adopt Einfeldt et al.'s method (4). A slight random perturbation of the relative order 10^{-15} is added to the downstream states. The upper and bottom boundary conditions are the outflow. The boundary conditions of the left and right side are the inflow and outflow respectively.

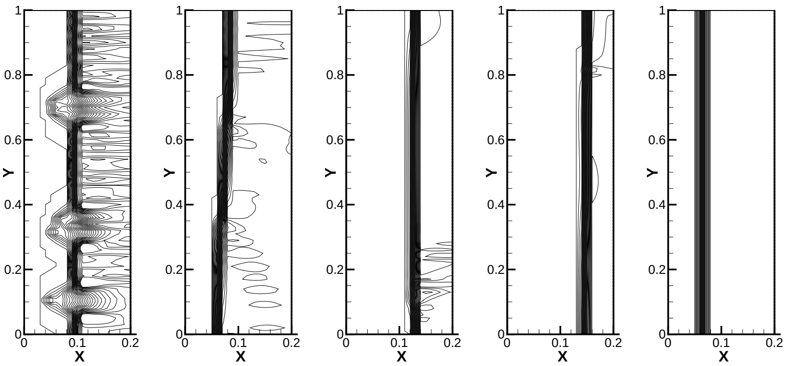

Figure 1. The density contours for 2D steady flow with Einfeldt et al.'s wave velocity estimates. The grid resolution is 20×100 cells. Thirty-one equally spaced contour lines from $\rho = 1$ to $\rho = 6$. From left to right: HLLEM, HLLC, HLLEC, HLLCM, HLLE. All of them are not stable.

For this one-dimensional shock problem, the shock wave front should remain stationary. The density contours using the schemes of HLLEM, HLLC, HLLEC, HLLCM and HLLE are displayed in Fig. 1. The shock positions in all schemes move and thus deviate from the correct steady state solution. Some move to the left and some to the right. Notice that this is a multi-dimensional phenomenon since such moving never been observed in a pure one-dimensional calculation(grid number is 1 in the y-direction). The carbuncle phenomenon has caused the normal shock to form a bulge which is unphysical.

Such solution behavior is a little surprising. It is well known that the HLLEM and HLLC flux are both able to exactly capture the contact and shear discontinuities, and thus they are susceptible to the carbuncle problem. But for the HLLEC, HLLCM and HLLE fluxes, the shear viscosities have been manipulated to the largest extend. These shear viscosities provide a kind of multi-dimensional dissipative mechanism on the face perpendicular to the shock, and they should suppress the drawbacks.

One knows that a good aspect ratio of the grid can alleviate the instability. If we add more cells in a direction normal to the shock, the anomalies should be cured partly. Fig. 2 illustrate the contour plots of density using the mesh with 40×100 cells. In this experiment, the first two fluxes still suffer from the carbuncle phenomena at once. For other schemes, the shock resolutions are enhanced and the sawtooth forms of the unstable mode disappear. However, the fluxes except the HLLE one still yield wrong shock velocity. For the HLLE flux, if we increase upstream mach number, for example, $M_a = 40$, the unstable phenomenon will appear again (not shown here). This numerical experiment shows that the refinement of the grid indeed plays an important role in alleviating numerical oscillation but does not cure the problem completely.

Clearly, the numerical experiments valid that there are at least two kinds of shock unstable mechanism in above numerical fluxes [8]. The primary one is due to lack of multi-dimensional dissipation in the shear direction of the shock. It can lead to the calculation collapse at once, just like the case in the HLLEM and HLLC schemes. The secondary might be from a kind of normal direction unstable mechanism of shock. We do not call it one dimensional unstable mode since such instability never been observed in pure one dimensional calculation. Such instability can be seen only when the multi-dimensional dissipation has been built in numerical flux, and results in wrong shock location, as shown in the fluxes of the HLLEC, HLLCM and HLLE.

In order to cure the second instability, we need add dissipation in one dimensional flux

IOP Conf. Series: Journal of Physics: Conf. Series **1290** (2019) 012026 doi:10.1088/1742-6596/1290/1/012026

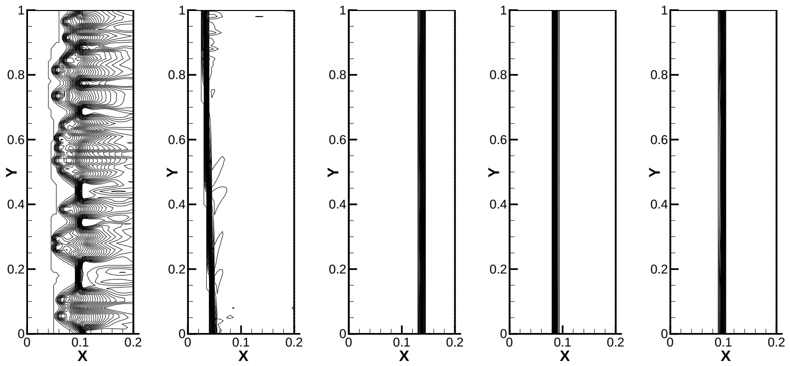

Figure 2. The density contours for 2D steady flow with Einfeldt et al.'s wave velocity estimates. The grid resolution is 40×100 cells. Thirty-one equally spaced contour lines from $\rho = 1$ to $\rho = 6$. From left to right: HLLEM, HLLC, HLLEC, HLLCM, HLLE.

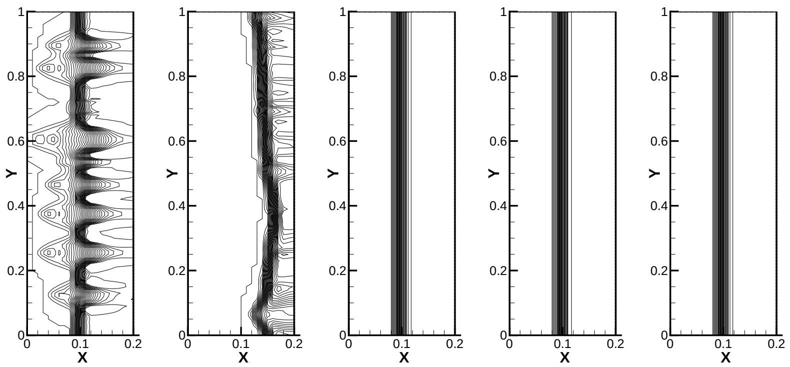

Figure 3. The density contours for 2D steady flow with Davis' wave velocity estimates. The grid resolution is 20×100 cells. Thirty-one equally spaced contour lines from $\rho = 1$ to $\rho = 6$. From left to right: HLLEM, HLLC, HLLEC, HLLCM, HLL(D). The last three fluxes are stable.

function. Here we adjust the signal velocities of the HLLC-type schemes.

Davis's wavespeeds algorithm [2] is expressed as

$$S_L = \min(u_L - a_L, u_R - a_R), \quad S_R = \max(u_L + c_L, u_R + c_R). \tag{16}$$

In general, the estimates are more diffusive than (4) since they can not distinguish an isolated shock.

The numerical results using Davis's estimates (16) are displayed in Fig. 3. The HLLC flux and HLLEM flux (we still use the same notations although different wavespeed estimates are adopted) suffer from catastrophic instability once more, while anomalous phenomena in the other fluxes disappear.

From above numerical experiments, we can draw some conclusions: the viscosity on the perpendicular cell face of shock wave is not high enough to damp out normal direction numerical instabilities. The grid refinement can modify bulge phenomenon but does not solve instability problem. A wavespeed algorithm which can crisply resolve shock seems to be vulnerable to the shock anomalies, and Davis's wave estimates have better performance in restraining instability.

4. A Linear Stability Analysis

In order to closer investigate the situation of shock instability, a kind of stability analysis method with shock structure [4] is used to illustrates stability mechanism of numerical scheme.

4.1. Matrix Stability Analysis

A matrix-based stability analysis [4] has been used to study the occurrence of unstable modes during the shock wave computation. Here we describe briefly the approach in [4] [15] for the convenience of discussion.

Similar to numerical experiments in preceding section. Calculations are performed on a 2D domain $[0,1]\times[0,1]$. The grid is composed of regular Cartesian cells without perturbation. The total cell number is $M = I \times J$.

For Einfeldt et al.'s algorithm, the initial steady shock states are (14) and (15) but with an equilibrium intermediate state,

$$\mathbf{W}^0_{i,j} = \begin{cases} \mathbf{W}_L, & i < I/2, \quad j = 1,\cdots,J, \\ \mathbf{W}_m, & i = I/2, \quad j = 1,\cdots,J, \\ \mathbf{W}_R, & i > I/2, \quad j = 1,\cdots,J, \end{cases} \tag{17}$$

where the intermediate state $\mathbf{W}_m$ locates on the Hugoniot curve based on the downstream state. This means

$$\begin{aligned} \rho_m &= \alpha_\rho \rho_L + (1-\alpha_\rho)\rho_R, \quad p_m = \frac{(\gamma+1)\rho_m - (\gamma-1)\rho_R}{(\gamma+1)\rho_R - (\gamma-1)\rho_m} p_R, \\ u_m &= u_R + (p_R - p_m)\left[\frac{2/\rho_R}{(\gamma-1)p_R + (\gamma+1)p_m}\right]^{1/2}, \quad v_m = 0, \end{aligned}$$

where $0 < \alpha_\rho \le 1$.

For the stability analysis of a steady field, we assume that

$$\mathbf{U}_{i,j} = \mathbf{U}^0_{i,j} + \delta\mathbf{U}_{i,j}, \tag{18}$$

where $\mathbf{U}^0_{i,j}$ is the conserved vector of $\mathbf{W}^0_{i,j}$ and $\delta\mathbf{U}_{i,j}$ is a small perturbation vector.

Substituting (18) into (2), and the numerical flux functions are linearized around the steady mean value, then we finally get the error evolution of all M cells in the domain,

$$\frac{d}{dt}\begin{pmatrix} \delta\mathbf{U}_{1,1} \\ \vdots \\ \delta\mathbf{U}_{I,J} \end{pmatrix} = S \begin{pmatrix} \delta\mathbf{U}_{1,1} \\ \vdots \\ \delta\mathbf{U}_{I,J} \end{pmatrix}, \tag{19}$$

where S is the stability matrix. Details can be referred to [4] and [15]. When considering only the evolution of initial errors, the solution of the linear time invariant system (19) is

$$\begin{pmatrix} \delta\mathbf{U}_{1,1} \\ \vdots \\ \delta\mathbf{U}^0_{I,J} \end{pmatrix} = \exp^{St} \begin{pmatrix} \delta\mathbf{U}^0_{1,1} \\ \vdots \\ \delta\mathbf{U}^0_{I,J} \end{pmatrix}. \tag{20}$$

The perturbation remains bounded only if the maximum of the real part of the eigenvalues of S is negative.

$$\max(Re(\lambda))) \le 0. \tag{21}$$

IOP Conf. Series: Journal of Physics: Conf. Series **1290** (2019) 012026 doi:10.1088/1742-6596/1290/1/012026

Remark 1. Different from Einfeldt et al.'s wave algorithm, Davis's wave speed estimates can not provide a single point equilibrium state to form a stationary shock wave. We obtain the stationary viscous profile $\mathbf{U}^0_{i,j}$ by a pure one-dimensional numerical calculation, whose initial value still adopts $\mathbf{W}^0_{i,j}$ in (17).

4.2. Analysis results
After obtaining numerical steady shock, we may carry out stability analysis for all the HLLE-type Riemann solvers. At first, we consider Einfeldt et al.'s algorithm.

By varying a parameter α_ρ, we check the stability of these solutions to perturbations. Just like pointed out by Dumbser et al. in [4], when $\rho_m \to \rho_L(\alpha_\rho \to 1)$, instability might occur. We represent stability domain of a flux function as $(0, \alpha_{\max})$ by the parameter α_ρ. The upper bounds $\alpha_{\max}$ of stability region depend on different numerical flux functions and strong shocks. They are listed in the Table 1.

Table 1. The upper bounds $\alpha_{\max}$ of stability region for Einfeldt et al.'s algorithm.

Mach	HLLEM	HLLC	HLLEC	HLLCM	HLLE
10	0.382	0.382	0.816	0.816	0.935
20	0.375	0.375	0.810	0.810	0.928
30	0.374	0.374	0.809	0.809	0.927
...					
100	0.373	0.373	0.808	0.808	0.926

Table 1 indicates clearly all flux formulae have unstable regions to perturbations, including the HLLE scheme. The upper bounds $\alpha_{\max}$ of the HLLEM flux are identical to those of the HLLC flux for same shock strength, and $\alpha_{\max}$ of the HLLEC scheme are the same as the HLLCM one. The ranking order is listed according to linear stability,

$$\text{HLLEM} = \text{HLLC} < \text{HLLEC} = \text{HLLCM} < \text{HLLE}.$$

With the increase of shock strength, the values of $\alpha_{\max}$ decrease, and this means the unstable region increases. A surprising finding is that the upper bounds have minor variations with the increase of upstream Mach number. We conjecture that there exists a common critical density jump to trigger local instabilities for different shock strengths.

Secondly, we implement a stability analysis for the HLLEC and HLLCM fluxes with initial parameter $\alpha_\rho = 0.81$. The maximal real parts of eigenvalues of stability matrix of the two fluxes (vs. upstream Mach number) are displayed in Fig. 4. The analysis shows that Davis's wavespeed estimates are stable for any strength of shock wave while Einfeldt et al.'s wavespeed estimates begin to destabilize with the increase of the upstream Mach number. Hence Davis's algorithm has better stability than Einfeldt et al.'s algorithm.

More analysis have been preformed but do not show here. For example, we employ Davis's wavespeed algorithm in x-direction flux and Einfeldt et al.'s in y-direction flux, or alternately, use Einfeldt et al.'s wavespeed algorithm in x-direction flux and Davis's in y-direction flux, then the stability of the hybrid fluxes are always the same as the single flux equipped with x-direction wavespeed algorithm. These results validate that the main factor to influence stability of the HLLEC and HLLCM fluxes comes from the nonlinear acoustic wave in normal direction, rather than comes from the insufficient viscosity in linear wave of transverse direction.

The mechanism why Davis's algorithm can provide more stable calculation than Einfeldt et al.'s algorithm is still not clear, but we try to understand it. From the first analysis, we know that if the state of the intermediate point ρ_m is sufficiently close to the downstream state, then

IOP Conf. Series: Journal of Physics: Conf. Series **1290** (2019) 012026 doi:10.1088/1742-6596/1290/1/012026

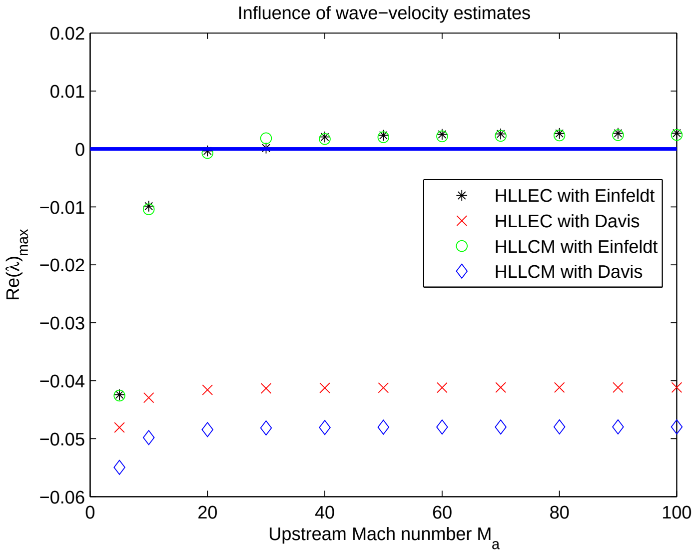

Figure 4. Maximal real part of eigenvalues of stability matrix vs. Mach number.

all Riemann solvers will be carbuncle free no matter how high the upstream Mach number. From the second analysis and numerical experiments, Davis's algorithm forces the intermediate point to be close to the downstream state, or deceases the density jump in the shock layer. The discussion of the concrete amount of the density jump in Davis's algorithm is beyond the scope of the article.

A natural question arises here: is Davis's wavespeed algorithm applicable for all strong shock waves? The reply depends on degree of density jump in a numerical shock layer. In an extreme case, the answer is no. In fact, Davis's wave speed estimates are not lower and upper bounds for the physical signal velocity, therefore it is possible to fail in shock calculations. It is worthwhile pointing out that Einfeldt et al. [5] stated incorrectly that (4) are lower and upper bounds for the physical signal velocity. Here we give an concrete case to demonstrate the limitation of two algorithms. Both of Einfeldt et al.'s algorithm and Davis's algorithm might underestimate the shock velocity.

Considering a Riemann problem with the following initial values,

$$\begin{aligned}\mathbf{W}_L &= (\rho_L, u_L, v_L, p_L, \gamma_L) = (1, 1, 0, 0, 3),\\ \mathbf{W}_R &= (\rho_R, u_R, v_R, p_R, \gamma_R) = (1, -1, 0, 0, 3).\end{aligned}$$

In this collision problem, the shock strength is infinite and the shock speed is 2. Note that the initial sound speed (in pre-shock) is 0, thus $S_L = \min(u_L, u_R) = -1$, $S_R = \max(u_L, u_R) = 1$ according to Davis's wavespeed algorithm. In addition, Roe average states $\hat{u} = 0, \hat{c} = 0$, thus S_L an S_R in Einfeldt et al.'s estimates are identical with Davis's estimates, which are smaller than the physical shock wave velocity.

Except such extreme cases, Davis's choice is rather robust in practice. We recommend this method in simulations to strong shock wave problems.

5. Conclusions

In this paper, we discuss the stability of some HLLE-type schemes when calculating strong shock wave problems. In particularly, we pay attention to those schemes which claimed to avoid carbuncle phenomenon. The conclusion about "only the eigenvalue associated to the linear vorticity mode is responsible for the instability" seems not correct [4]. All HLLE-type Riemann solvers, including those are believed to be free carbuncle anomalies, suffer from severe instability. Nonlinear acoustic waves rather than linear vorticity and shear waves play an important role to damp out instability.

A linear stability analysis shows that Einfeldt et al.'s algorithm, which is able to capture an isolated shock exactly, is more susceptible to the carbuncle problem. While Davis's estimates have more dissipation and hence may overcome such numerical instability. We recommend to use the simple David's wave estimates when calculating strong shock wave problems, although the algorithm has its limitation in some extreme situations.

Acknowledgments
This project was supported by the National Natural Science Foundation of China (U1630249, 11871112, 11471048), the Science Challenge Project (No. JCKY2016212A502) and the Foundation of LCP.

References

[1] Batten P, Clarke N, Lambert C and Causon D M 1997 *SIAM J. Sci. Comput.* **18** 1553-70
[2] Davis S F 1988 *SIAM J. Sci. Stat. Comput.* **9** 445-73
[3] Dukowicz J K, Meltz B 1992 *J. Comput. Phys.* **99** 115-34
[4] Dumbser M, Morschetta J M, Gressier J 2004 *J. Comput. Phys.* **197** 647-70
[5] Einfeldt B, Munz C D, Roe P L, Sjogreen B 1991 *J. Comput. Phys.* **92** 273-95
[6] Harten A, Lax P D and van Leer B 1983 *SIAM Rev.* **25** 35-61
[7] Harten A 1983 *J. Comput. Phys.* **49** 357-93
[8] Kitamura K, Roe P L, and Ismail F 2009 *AIAA Journal*, **47** 44-53
[9] Pandolfi M and D'Ambrosio D 2001 *J. Comput. Phys.* **166** 271-301
[10] Park S H, Kwon J H 2003 *J. Comput. Phys.* **188** 524-42
[11] Peery K M and Imlay S T 1988 *AIAA Paper* 88-2924
[12] Quirk J 1994 *Int. J. Numer. Meth. Fluid.* **18** 555-74
[13] Rider W J 2000 *J. Comput. Phys.* **162** 395-410
[14] Sanders R, Morano E and Druguet M C 1998 *J. Comput. Phys.* **145** 511-37
[15] Shen Z J, Yan W and Yuan G W 2014 *Commun. Comput. Phys.* **15** 1320-42
[16] Shen Z J, Yan W and Yuan G W 2016 *J. Comput. Phys.* **309** 185-206
[17] Toro E F 1997 *Riemann Solvers and Numerical Methods for Fluid Dynamics* (Berlin: Springer)
[18] Toro E F, Spruce M, Speares W 1994 *Shock Wave* **4** 25-34
[19] Xie W J, Li W, Li H, Tian Z. Y, Pan S 2017 *J. Comput. Phys.* **350** 607-37
[20] Xu K, Hu J 1998 *J. Comput. Phys.* **142** 412-27